Desalination and Water Treatment
www.deswater.com
doi: 10.1080/19443994.2013.800287

52 (2014) 3085–3095
April

Taylor & Francis
Taylor & Francis Group

Oil removal in a biosorption column using immobilized *M. rouxii* biomass

Asha Srinivasan[a], Thiruvenkatachari Viraraghavan[b,*]

[a]*Opus DaytonKnight Consultants Ltd., North Vancouver and University of British Columbia, Vancouver, BC, V6T1Z4, Canada*
[b]*Faculty of Engineering and Applied Science University of Regina, Regina, SK, S4S0A2, Canada*
Email: t.viraraghavan@uregina.ca

Received 29 August 2012; Accepted 22 April 2013

ABSTRACT

A continuous column study was carried out using immobilized *Mucor rouxii* biomass beads as a biosorbent for the removal of oil from water. Three oils were used in the study—standard mineral oil, canola oil, and Bright-Edge 80 cutting oil. Column data were examined using Thomas, Yan, Yoon–Nelson, Wolborska, Belter, and Chu models. Thomas, Yan, and Yoon–Nelson models were found suitable for describing column behavior for all the three oils studied. The sorbed oil was desorbed from the beads using deionized water. After column regeneration, the beads could be reused to remove oil to the extent of initial capacity.

Keywords: Biosorption; Oil; *Mucor rouxii*; Breakthrough; Column

1. Introduction

Rapid urbanization and urban development cause an annual increase in the discharge of oil-containing wastewater to the environment. Oils that are found in contaminated waters can be fats, lubricants, cutting liquids, heavy hydrocarbons (tars, grease, crude oils, and diesel oil), and light hydrocarbons (kerosene, jet fuel, and gasoline). Major industrial sources of oily wastewater include petroleum refineries, metal manufacturing and machining, and food processors. The presence of emulsified oil in wastewaters is of real concern as it often results in fouling of process equipment and creates problems during biological treatment of such wastewaters [1].

Biomass of fungus *Mucor rouxii* is a type of biomaterial, which has been used for many applications in separation technology. *M. rouxii* is a filamentous fungus in which chitosan is the most abundant component of the cell wall. Separately, chitosan, in the form of powder and flakes, was found to significantly adsorb oil from water [2,3]. Large quantities of positively charged chitosan and negatively charged phosphate and glucouronic acid on the cell wall of *M. rouxii* have been found to offer extensive possibilities for binding heavy metals [4]. No detailed work has been conducted so far on the removal of oil from water by nonviable fungal adsorbents, although, a few studies have been conducted on uptake of oil by live fungi [5,6]. Recently, Srinivasan and Viraraghavan [6] conducted preliminary batch studies on biosorption of oil by nonviable fungal biomass *M. rouxii* and found that the biomass had a strong potential to remove various oils from water. Detailed batch studies on oil adsorption were further conducted using powdered

*Corresponding author.

nonviable *M. rouxii* biomass. However, no study has been conducted so far to remove oil using fungal biomass in a fixed bed column. The use of dead biomass in powdered form in a fixed bed column has limitations, such as difficulty in the separation of biomass after adsorption, mass loss after regeneration [7,8], low strength, and small particle size [9]. The dead biomass has to be immobilized in a granular or polymeric matrix to improve the mechanical strength of the biosorbent.

In a granular medium such as immobilized biomass beads, the possible separation/breakdown mechanisms for oil in water are filtration, coalescence, and adsorption. In order to understand the contribution of coalescence and filtration mechanisms, Srinivasan et al. [10] used immobilized *M. rouxii* biomass as a granular medium in a fixed bed column to breakdown an oil-in-water emulsion. The study revealed that the Carman–Kozeny filtration equation predicted the pressure drop across the bed for both single- and two-phase flows fairly well. Further, the coalescence efficiency of the immobilized biomass bed using standard mineral oil (SMO)-in-water emulsion was evaluated to be only 15.9%. The low coalescence efficiency obtained could be attributed to high stability of the SMO emulsion that was chemically stabilized using emulsifiers in the study. Hence, there is a need to study the contribution of adsorption in removing oil in a fixed bed column using immobilized *M. rouxii* biomass. The method that can be used to estimate the oil adsorption capacity and adsorption kinetics in a fixed bed column is through the breakthrough curve. Such a study is needed to develop design data for a fixed bed adsorber. Hence, the objective of the present investigation was to examine the removal of oil from water in a column using immobilized *M. rouxii* biomass beads and to model the breakthrough data using kinetic models.

2. Methods

2.1. Experimental materials

The fungal strain *M. rouxii* was purchased from American Type Culture Collection (ATCC), Rockville, Maryland, USA (ATCC #24905). The following oils were used in the study:

(1) SMO (light) marketed by Fisher Scientific Company, USA, emulsified with oleic acid and triethanolamine using Regina tap water according to the procedure used by Biswas [11].
(2) Vegetable oil, Canola oil (CO) marketed in Canada, emulsified in the same manner as SMO.
(3) DoALL Bright-Edge 80, a cutting oil manufactured by DoALL Company, IL, USA, emulsified in the same manner as SMO.

The characteristics of the three oils used and *M. rouxii* biomass are given in Table 1.

2.2. Preparation of nonviable fungal biomass

M. rouxii strain was routinely maintained on potato dextrose agar plates. It was grown aerobically by shake flask method. It was cultivated using a growth medium comprising of yeast extract (3 g/L), peptone (10 g/L), and glucose (replaced by dextrose) (20 g/L) [13,14]. The pH of the growth medium was maintained at 4.5 by 1.0 N HCl. The culture was grown in an aerobic condition at room temperature (22 ± 2 °C) with 100 mL of the liquid medium in 250 mL conical flasks on a rotary shaker agitated at 125 rpm. *M. rouxii* was harvested after three days of growth by filtering the growth medium through a 150 μm sieve. The harvested fungal biomass was washed with generous amounts of deionized water and autoclaved for 30 min at 121 °C and 103 kPa. The autoclaved biomass was allowed to cool down and dried in an oven at 60 °C for 24 h. The dried biomass was powdered into a fine size using a grinder. The biomass passing through 400-micronmesh sieve was used for the experiment.

2.3. Immobilization of biomass

Powdered *M. rouxii* biomass was immobilized in a polysulfone matrix following the procedure described by Kapoor and Viraraghavan [7], but with certain changes. Seven grams of powdered pretreated biomass and 7 g of polysulfone were mixed in 100 mL of *N*,*N*-dimethyl formamide (DMF). The beaker was immediately sealed to avoid volatilization of DMF and then shaken for approximately 16 h on a magnetic shaker for polysulfone to completely dissolve in DMF and form a slurry of uniform consistency. The slurry was sucked into a 10 mL syringe and allowed to drop slowly into a tub of deionized water. Due to the consistency of the slurry and the contact with the air for a brief moment, spherical droplets formed beads upon contact with deionized water in the tub. The biomass was thus immobilized within the solidified polysulfone matrix. The beads were cured in a moderately agitated deionized water bath for 24 h to diffuse out the DMF. After curing, the beads were air dried for three days at room temperature (22 ± 2 °C). A sieve analysis of the immobilized biomass beads was

Table 1
Characteristics of the three oils and *M. rouxii* biomass

Characteristics of oils[a]			
Type of oil	Density (kg/m^3)	Viscosity (Pa.S)	Interfacial tension (dynes/cm)
SMO	841.9	0.143	5.3
Canola oil	913.2	0.070	3.1
Bright-Edge 80	821.5	0.023	2.7
Characteristics of *M. rouxii*[b]			
pH	6.4		
Moisture content (%)	4.6		
Porosity (%)	85		
Surface area (m^2/g)	20.55		
Color	Light brown		
Chemical analysis (% by weight)	Chitosan—32.7		
	Chitin—9.4		
	Lipids—7.8		
	Fucose—3.8		
	Mannose—1.6		
	Galactose—1.6		
	Protein—6.3		
	Phosphate 23.3		
	Magnesium—1.0		
	Calcium—1.0		
	Glucuronic acid—11.8		

[a]Characteristics of the three oils taken from Srinivasan and Viraraghavan [12].
[b]Composition of *M. rouxii* cell wall was obtained from Bartnicki-Garcia and Nickerson [13].

conducted with the use of sieves of sizes 2.36, 2.0, 1.18, 0.85, 0.6, and 0.42 mm. Beads with an irregular shape and beads smaller than 0.42 mm or bigger than 2.36 mm were discarded.

2.4. Continuous breakthrough studies

Immobilized biomass beads (4.5 g) were packed into a plastic column 1.27 cm in diameter and 45 cm in height, with a bed depth of 30 cm. Glass beads were placed on both ends of the column (height of 1 cm), to allow for even distribution of the influent and also to prevent the biomass beads from floating. Glass wool was placed between the glass beads and the biomass beads at the bottom of the column. The column was sealed at the bottom using a rubber stopper with a single bore. Tygon tubing was used for the connections. The empty bed contact time was 15 min. The oil-in-water emulsion was fed by a peristaltic pump through the column at a flow rate of 2.6 mL/min. The initial concentration of the oil was 50 mg/L. The initial pH of all three oil-in-water emulsions was in the range of 7.5–7.6 and in the effluent it was in the range of 7.0–7.3. Effluent samples were collected at regular time intervals. The effluent oil concentrations were measured using Horiba OCMA-350 oil content analyzer. Horiba OCMA-350 has an inbuilt NDIR spectrophotometer and displays oil concentration directly in mg/L on a digital panel. Oil was extracted with tetrachloroethylene (ultra-resi analyzed) before being analyzed by OCMA-350. Once the ratio of effluent to influent concentration reached a value of approximately 0.95 or higher, the column study was terminated. At this point, the column was considered to have reached exhaustion.

2.5. Column regeneration and reuse

After the column reached exhaustion, the column saturated with oil was eluted using DI water to desorb oil from beads. Samples were collected at regular time intervals to measure the concentration of oil in the effluent. Then, the column was fed again with the same oil-in-water emulsion with a concentration of 50 mg/L oil under similar experimental conditions as that of the initial run for the second cycle of operation to investigate the potential of reusing the beads for oil

removal. Effluent oil samples were collected at regular time intervals.

2.6. Model of column data

The successful design of a column adsorption process requires the prediction of the concentration-time profile or breakthrough curve for the effluent. A number of mathematical models have been developed to describe the concentration time profile in order to assist in the design. In general, mechanisms operating in a biosorption column involve axial dispersion in the direction of the liquid flow, film diffusion resistance, and intraparticle diffusion resistance which may include both pore and surface diffusion, and sorption kinetics at the adsorbent surface [15,16]. Nonlinearity, associated with equilibrium expressions, leads to sets of partial differential equations that may require a complicated numerical solution. In addition, independent experiments may be required to estimate the numerous equilibrium, transport, and sorption kinetic parameters involved [15]. Otherwise, multiparameter fitting of breakthrough curves may reduce the physical significance of the mechanistic parameters [16]. Obtaining a numerical solution with current computing facilities may no longer be rigorous but semi-emperical or approximate methods are still extensively used to simulate breakthrough curves of adsorption columns [17].

The goal of this research is to model the breakthrough behavior of the fixed bed column with decided accuracy. Different kinetic models, useful in process design, can be fitted to the column data to determine the characteristic parameters of the column. The Thomas model is widely used to evaluate column performance. The breakthrough curves for oil adsorption in a fixed bed column using different sorbents have been predicted using the Thomas model [18–20]. Five kinetic models were fitted to the column data to predict breakthrough curves: Thomas, Yan, Belter, Chu, Yoon–Nelson, and Wolborska models. The breakthrough curve for the second run of operation was fitted to Thomas model. Nonlinear regression was performed with the statistical software STATISTICA for Windows [21].

2.6.1. The Thomas model

The Thomas model is used to predict the breakthrough curve and the maximum solute uptake by an adsorbent. Data collected through breakthrough experiments were fitted to the Thomas model by nonlinear regression analysis performed with the statistical software STATISTICA for Windows [21]. The Thomas model [22] has the following form [23]:

$$\frac{C_e}{C_o} = \frac{1}{1 + (K_T/Q\{q_o m - C_o V\})} \tag{1}$$

where C_e is the effluent adsorbate concentration (mg/L); C_o the influent adsorbate concentration (mg/L); K_T the Thomas rate constant (L/min mg); q_o the maximum solid phase concentration of the solute (mg/g); m the mass of the adsorbent (g); V the throughput volume (mL); and Q is the volumetric flow rate (mL/min).

2.6.2. The Yan model

Column kinetics in a biosorption column was described more adequately by a modified dose–response model proposed by Yan et al. [24] than the Thomas model. The model was developed for heavy metal removal in a biosorption column and is used to describe the binary response regression problem. The logistic equation is expressed as follows:

$$\frac{C_e}{C_o} = 1 - \left[\frac{1}{1 + \{V/d\}^a}\right] \tag{2}$$

where d is the throughput volume that produces same C_e/C_o value at 50% removal and a is the constant, denoting the slope of the function.

2.6.3. The Belter and Chu models

The models used in this study were the ones developed by Belter et al. [25] (Eq. (3)) and modified by Chu [15], as it is shown in Eqs. (4) and (5).

$$\frac{C_e}{C_o} = \frac{1}{2}\left(1 + \mathrm{erf}\left[\frac{t - t_o}{\sqrt{2}\sigma t_o}\right]\right) \tag{3}$$

$$\frac{C_e}{C_o} = \frac{1}{2}\left(1 + \mathrm{erf}\left[\frac{(t - t_o)\ \exp(-\sigma(t/t_o))}{\sqrt{2}\sigma t_o}\right]\right) \tag{4}$$

$$\frac{C_e}{C_o} = \frac{1}{2}\left(1 + \mathrm{erf}\left[\frac{(t - t_o)\ \exp(-\sigma(t/t_o))}{\sqrt{2}\sigma t_o}\right]\right) \tag{5}$$

where erf (x) is the error function of x, t the residence time inside the column, and t_0 the temporal parameter which indicates time needed for the outlet metal concentration to be the half of the one inlet metal concentration and σ is the standard deviation which is a measure of the slope of the breakthrough curve. The model parameters t_0 and σ can be estimated by fitting

Eqs. (4) and (5) to experimental breakthrough data. Matlab was used for the mathematical solution of the above equations.

2.6.4. The Yoon and Nelson model

Yoon and Nelson [26] have developed a relatively simple model addressing the adsorption and breakthrough of adsorbate vapors or gases with respect to activated charcoal. The Yoon and Nelson equation related to a single-component system is expressed as:

$$\ln\frac{C}{C_o - C} = K_{YN}t - t_{1/2}K_{YN} \tag{6}$$

where K_{YN} is the rate constant (min^{-1}); $t_{1/2}$, the time required for 50% adsorbate breakthrough (min), and t is the breakthrough time (min). The values K_{YN} and $t_{1/2}$ may be determined from a plot of ln $C/(C_o - C)$ vs. sampling time (t) according to Eq. (6). If the theoretical model accurately characterizes the experimental data, this plot will result in a straight line with slope of K_{YN} and intercept K_{YN} $t_{1/2}$.

2.6.5. The Wolborska model

The Wolborska [27] model generally describes the concentration distribution in the bed for the low concentration region (low C/C_o) of the breakthrough curve:

$$\ln\frac{C}{C_o} = \frac{\beta_a C_o}{N_o}t - \frac{\beta_a Z}{U_o} \tag{7}$$

where β_a is the kinetic coefficient of the external mass transfer (min^{-1}), N_o saturation concentration in the Wolborska model (mg/L), U_o superficial velocity (mm/min), and Z height of the column (mm). The expression of the Wolborska model is equivalent to the Adams–Bohart model if the coefficient k is equal to β_a/N_o. So, the parameters in these two models can be determined from a plot of ln (C/C_o) against t at a given bed height and flow rate.

3. Results and discussion

The sieve analysis of the beads showed that the size of the majority of the beads ranged from 0.42 to 2.36 mm. The coefficient of uniformity C_u of the beads could be calculated using the following equation:

$$C_u = \frac{D_{60}}{D_{10}} \tag{8}$$

where D is the diameter of the particles and the subscript (10, 60) refers to the percent that is smaller. D_{10} also denotes the effective size of the particles. Results showed that the value of C_u was 1.71, the effective size of the beads was 1.28 mm, and the average particle size was 2.11 mm. Bed volume was calculated by the following equation:

$$\text{Bed volume} = t \times q/V_b \tag{9}$$

where t is run time (min), q is flow rate (mL/min), and V_b is the product of cross-sectional area of column and bed height (cm^3) = 37.98 cm^3. Breakthrough curves for biosorption of SMO, CO, and Bright-Edge 80 on the immobilized beads are shown in Fig. 1. The breakthrough experiments lasted 42, 24, and 30 h for SMO, CO, and Bright-Edge 80, respectively. The pH in the effluent was in the range of 7.0–7.3 from the start to the end of the operation. The column was able to remove 50% of oil in approximately, 28, 22, and 24 bed volumes for SMO, CO, and Bright-Edge 80, respectively. The bed exhaustion ($C/C_o \geqslant 0.95$) occurred at 172, 90, and 98 bed volumes for SMO, CO, and Bright-Edge 80, respectively.

3.1. The Thomas model

Data were fitted to the Thomas equation model through the use of non-linear regression analysis to determine the maximum solid-phase concentration (q_o) with the aid of software package STATISTICA (Release 5.0). The equation parameters such as K_T and q_o values are shown in Table 2. From the high correlation coefficient ($r > 0.95$) and the t statistical significance at the 95% confidence level, it can be said that the Thomas equation could describe the breakthrough data reasonably. The Thomas model was derived from the equation of mass conservation in a flow system [22]. The model is developed based on the assumption that the rate driving force obeys second-order reversible reaction kinetics, and the adsorption equilibrium follows the Langmuir model with no axial dispersion [22]. Based on the q_o values obtained for Thomas model, the adsorption capacity of oil on the immobilized *M. rouxii* beads were 14.67, 9.87, and 10.67 mg/g for SMO, CO, and Bright-Edge 80, respectively. The maximum solid phase concentrations were based on the mass of beads. If these were based on the biomass mass, the maximum solid phase concentration would be two times higher than the values shown above as the bead composition consisted of 50% biomass and 50% polysulfone. Thus, q_o values based on the mass of biomass would be 29.34, 19.74, and 21.34 mg/g for

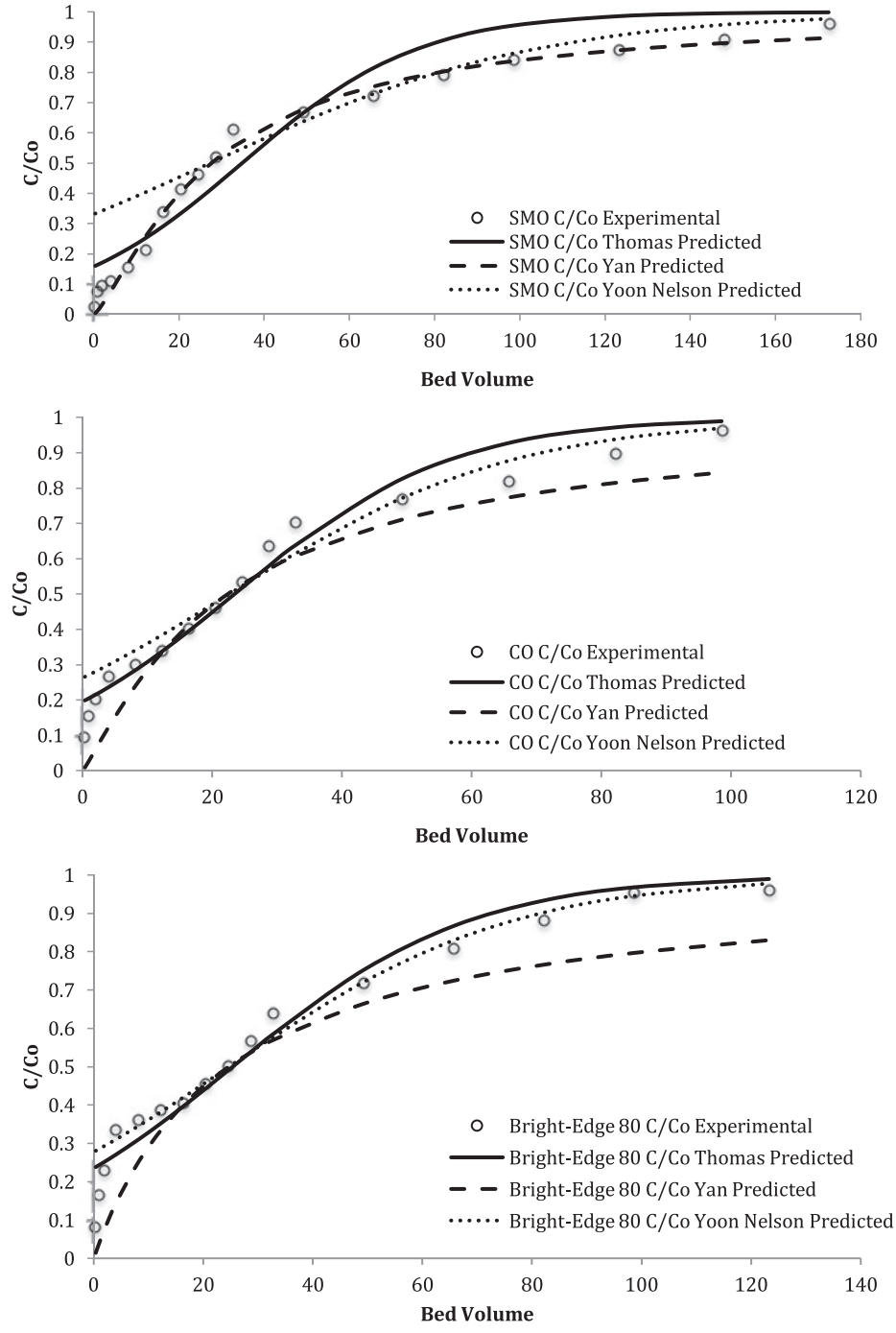

Fig. 1. Breakthrough curves for SMO, CO, and Bright-Edge 80.

SMO, CO, and Bright-Edge 80, respectively. Uptake of oil by adsorbents such as organo-clay/anthracite mixture [19] and vermiculite [20] was found to be well described by the Thomas model. The values of the Thomas constants from column studies using other sorbents for oil removal are given in Table 3. The adsorption capacity (q_o) values calculated from the Thomas model imply that immobilized *M. rouxii* biomass showed higher oil adsorption capacity than vermiculite for both SMO and CO. Adsorption capacity of SMO by immobilized *M. rouxii* biomass and organoclay/anthracite mixture was comparable. However, the adsorption capacity of SMO by horticultural peat was higher than that of immobilized

Table 2
Parameters calculated using kinetic models

Model	SMO		CO		Bright-Edge 80	
	Constants	r	Constants	r	Constants	r
Thomas	$K_T = 7x10^{-5}$ L/min mg $q_o = 14.67$ mg/g	0.95	$K_T = 8.3 \times 10^{-5}$ L/min mg $q_o = 9.87$ mg/g	0.98	$K_T = 6 \times 10^{-5}$ L/min mg $q_o = 10.67$ mg/g	0.97
Yan	a = 1.29	0.99	a = 1.29	0.95	a = 0.98	0.95
Belter	$t_o = 520$ min $\sigma = 0.98$	0.92	$t_o = 347.1$ min $\sigma = 1.17$	0.96	$t_o = 376.7$ min $\sigma = 1.39$	0.95
Chu form 1 (Eq. (4))	$t_o = 410.5$ min $\sigma = 0.84$	0.81	$t_o = 381.8$ min $\sigma = 1.19$	0.82	$t_o = 405.2$ min $\sigma = 1.36$	0.74
Chu form 1 (Eq. (5))	$t_o = 420$ min $\sigma = 0.46$	0.93	$t_o = 311.6$ min $\sigma = 0.49$	0.86	$t_o = 338$ min $\sigma = 0.48$	0.76
Yoon Nelson	$K_{YN} = 0.002$ min^{-1} $t_{1/2} = 775$ min	0.91	$K_{YN} = 0.003$ min^{-1} $t_{1/2} = 406$ min	0.96	$K_{YN} = 0.003$ min^{-1} $t_{1/2} = 424$ min	0.96
Wolbroska	$\beta_a = 0.16$ min^{-1} $N_o = 2058.8$ mg/L	0.87	$\beta_a = 0.11$ min^{-1} $N_o = 2{,}143$ mg/L	0.90	$\beta_a = 0.1$ min^{-1} $N_o = 2{,}292$ mg/L	0.95
Second run (after regeneration) Thomas	$K_T = 1.4 \times 10^{-4}$ L/min mg $q_o = 2.54$ mg/g	0.91	$K_T = 1.1 \times 10^{-4}$ L/min mg $q_o = 0.03$ mg/g	0.90	$K_T = 1.05 \times 10^{-4}$ L/min mg $q_o = 0.49$ mg/g	0.9

Note: r-correlation coefficient. All model parameters statistically significant (t-test) at 95% confidence level.

M. rouxii biomass, which may be attributed to the fibrous nature of peat. The Thomas model rate constant (K_T) for SMO was 27.6, 1132.6, 0.339, and 4,200 L/h-kg for horticultural peat, organoclay/anthracite, vermiculite, and immobilized *M. rouxii* biomass, respectively.

3.2. The Yan model

The value of maximum solid phase concentration of solute (q_o) obtained from the Yan's model based on the immobilized *M. rouxii* bead mass were 11.6, 9.4, and 10.4 mg/g for SMO, CO, and Bright-Edge 80, respectively. The q_o value based on the mass of biomass would be 23.2, 18.8, and 20.8 mg/g for SMO, CO, and Bright-Edge 80, respectively. The q_o values predicted by Thomas model were slightly higher than the ones predicted by Yan model for all the three oils. Yan's empirical model is developed to minimize the error resulting from use of the Thomas model, especially at lower or higher time periods of the breakthrough curve. High correlation coefficient ($r > 0.95$) values and t statistical significance at 95% confidence level were obtained for Yan model. This showed that Yan model described the breakthrough curves with great accuracy. The values of the empirical constant "*a*" and correlation coefficient for the three oils are given in Table 2. The limitation of the Yan model is that it may be difficult to relate the empirical parameter "*a*" with the experimental conditions, so the scale up of the system may be difficult [28].

3.3. The Belter and Chu models

Experimental data were fitted to the mathematical models proposed by Belter et al. [25] and Chu [11] in Fig. 2. Eqs. (4) and (5) were modified from Eq. (3) by Chu [15] so that the experimental data would fit better even if the breakthrough curve is symmetrical or asymmetrical. The Belter model is capable of describing only a symmetric breakthrough curve behavior. The process variables such as the flow rate, bed height, and average size of the sorbent were not used to develop Eq. (3) and it is necessary to empirically correlate the two model parameters with these variables [15].

The model parameters σ and t_o and the correlation coefficient (r) values obtained for the three oils are shown in Table 2. For all the three oils, the breakthrough curve showed a good fit to the model described by Eq. (3) with r^2 values higher than 0.92 at 95% confidence level. The model equation employed by Chu in Eq. (5) (with the negative sign in exponential term) fitted better than Eq. (4) (with the positive sign in exponential term) for all the three oils. In the case of SMO, the breakthrough curve was well

Table 3
Comparison of Thomas constants for other oil sorbents

Oil	Adsorbent used as medium	Influent concentration, mg/L	Effluent concentration, mg/L	Mass of adsorbent, kg/ Bed depth, m	Flow rate, mL/min	Breakthrough volume, L	K_T, L/h-kg	q_0, kg/kg	Reference
SMO	Horticultural peat	217.9	83.9	0.175/0.3	50	782	27.6	1.58	[18]
MCO	Horticultural peat	210.0	186.9	0.175/0.3	50	1,080	30.2	1.33	[18]
CUT	Horticultural peat	278.2	205.3	0.175/0.3	25	120	32.4	0.14	[18]
RE	Horticultural peat	8.9	8.3	0.175/0.3	25	480	210.0	0.03	[18]
PW	Horticultural peat	38.4	37.2	0.175/0.3	50	810	85.9	0.19	[18]
SMO	Organolcay/ anthracite	46	44.1	0.225/1	12	47.5	1132.6	0.0025	[19]
KUT	Organolcay/ anthracite	49	44.3	0.225/1	12	34.6	1748.2	0.0014	[19]
VAL	Organolcay/ anthracite	51	48.0	0.225/1	12	30.2	9327.7	0.0008	[19]
RE	Organolcay/ anthracite	8.3	5.9	0.225/1	12	95.0	3891.5	0.0019	[19]
SMO	Vermiculite	47	42.8	0.016/0.2	12	8.64	0.339	0.0012	[20]
CO	Vermiculite	45	40.5	0.016/0.2	12	8.64	0.077	0.0077	[20]
KUT	Vermiculite	30	27.3	0.016/0.2	12	14.4	0.17	0.0061	[20]
RE	Vermiculite	10.6	9.8	0.016/0.2	12	14.4	0.079	0.0027	[20]
SMO	Immobilized *M. rouxii*	50	48	0.0045/0.3	2.6	6.55	4,200	0.0099	This study
CO	Immobilized *M. rouxii*	50	48.1	0.0045/0.3	2.6	3.74	4,980	0.0147	This study
Bright-Edge 80	Immobilized *M. rouxii*	50	48.2	0.0045/0.3	2.6	4.68	3,600	0.0107	This study

Note: MCO—Midale crude oil; CUT—Cutting oil, RE—Refinery effluent; PW—Produced water; KUT—Kutwell 45 oil; VAL—Valcool oil. All model parameters statistically significant (*t*-test) at 95% confidence levels.

described by both Eqs. (3) and (5) showing a high r^2 value (>0.92) at 95% confidence interval. In the case of all the three oils, the model in Eq. (5) underestimates the effluent oil concentration, while the model in Eq. (4) overestimates the experimental values. In addition, Eqs. (3) and (4) predict a nonzero effluent concentration at $t = 0$ which contradicts real conditions for all the three oils. The shape of the curve predicted by Eq. (4) is different from the ones predicted by other model equations. A similar pattern of breakthrough curve was observed by Chu for Eq. (4) and suggested the curve is a result of Eq. (4) over-estimating the sharpness of the leading and trailing edges of the breakthrough curve [15]. However, using these simple models to design or optimize fixed bed biosorption columns requires knowledge of the effect of process variables on the two model parameters, t_o and σ [15].

3.4. The Yoon and Nelson model

A simple theoretical model developed by Yoon–Nelson was applied to investigate the breakthrough behavior of the three oils on immobilized biomass beads. This model is based on the assumption that the rate of decrease in the probability of adsorption for each adsorbate molecule is proportional to the probability of adsorbate adsorption and the probability of adsorbate breakthrough on the adsorbent. The values of K_{YN} and $t_{1/2}$ are listed in Table 1. The experimental data were similar to those predicted by the

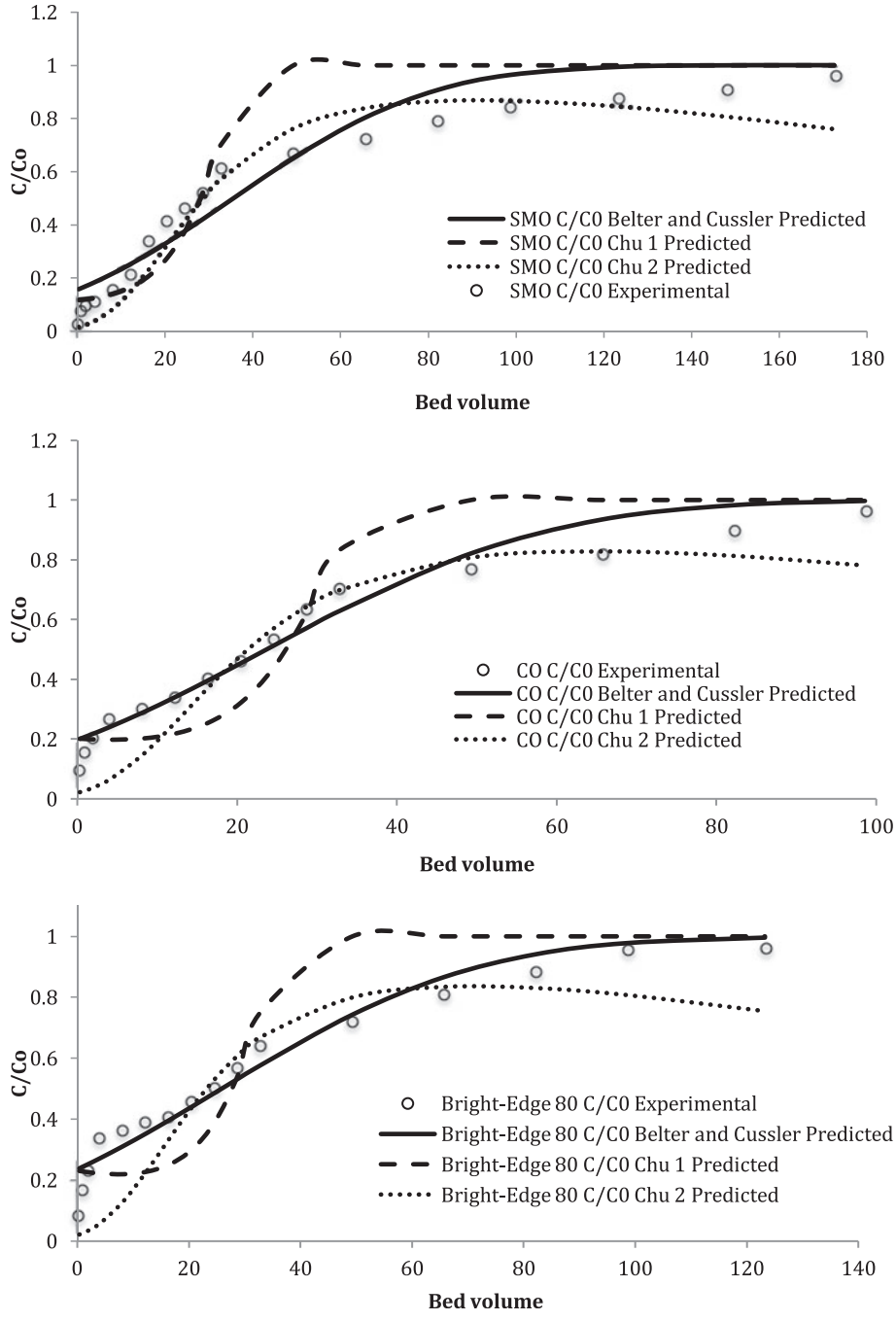

Fig. 2. Breakthrough curves for the three oils predicted by the Belter and Chu models.

Yoon–Nelson model in the C/C_o region from 0.4 to 0.97 for all the three oils. Both CO and Bright-Edge 80 showed high correlation values ($r > 0.95$) and the correlation was statistically significant (from t-test) at the 95% confidence level. The model equations obtained with the nonlinear regression analysis of Yoon Nelson model could describe the breakthrough data better for CO and Bright-Edge 80.

3.5. The Wolborska model

The Wolborska sorption model was applied to experimental data for the description of the initial part of the breakthrough curve. This approach was focused on the estimation of characteristic parameters, such as maximum sorption capacity (N_o) and kinetic coefficient of the external mass transfer (β_a). After applying Eq. (9) to the experimental data, a linear relationship

between ln (C/C_o) and t was obtained for ln $(C/C_o) < -0.3$, for all three-breakthrough curves ($r \geqslant 0.85$). The breakthrough curves for SMO and CO showed high correlation coefficient ($r > 0.9$) at 95% confidence interval. Respective values of N_o and β_a calculated from the ln(C/C_o) vs. t plots for the three oils studied are presented in Table 1. This showed that the overall system kinetics was dominated by external mass transfer in the initial part of sorption in the column. The kinetic coefficient β_a reflects the effect of both mass transfer in liquid phase and axial dispersion. Wolborska observed that in short beds or at high flow rates of solution through the bed, the axial diffusion is negligible and $\beta_a = \beta_o$, the external mass transfer coefficient. Although the Wolborska model provides a simple and comprehensive approach to running and evaluating sorption-column tests, its validity was limited to the range of the used conditions. The expression of the Wolborska model is equivalent to the Adams–Bohart relation [29] if the coefficient K_{AB} is equal to β_a/N_o.

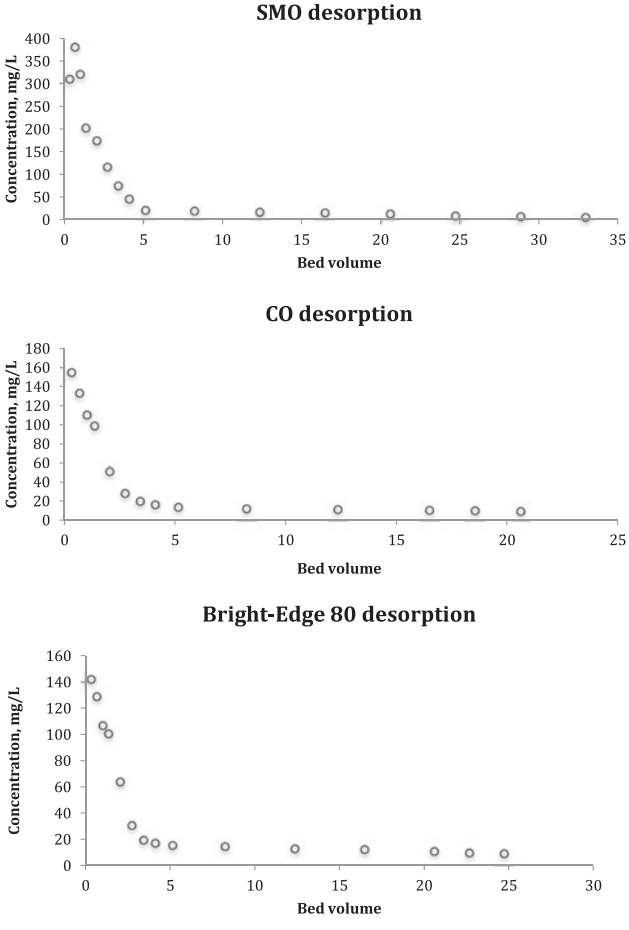

Fig. 3. Desorption profile for the three oils using deionized water.

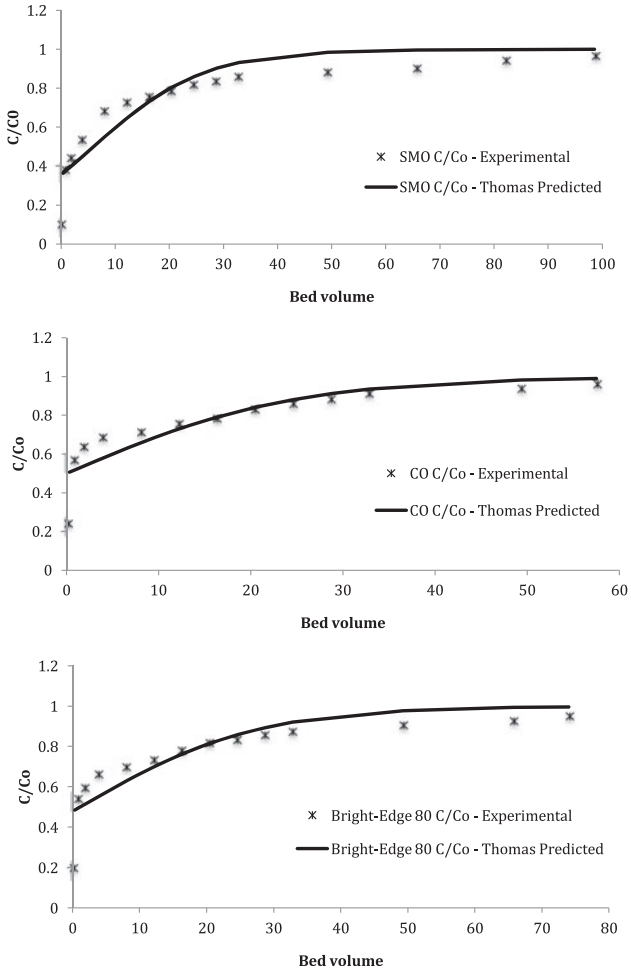

Fig. 4. Breakthrough curve for the three oils for the second run.

3.6. Column regeneration and reuse

Concentrations of oil in elutant for columns that had been fed with the three oils, respectively, are shown in Fig. 3. The results showed that the adsorbed oils could be desorbed from the beads in the column. Desorption produced no visible effects on the physical properties of the beads. SMO, CO, and Bright-Edge 80 were desorbed from the column in 32, 20, and 24 bed volumes, respectively. It should be noted that oil desorption was achieved at much higher level in the initial two bed volumes. Maximum oil concentrations of 380, 154, and 142 mg/L were obtained for SMO, CO, and Bright-Edge 80, respectively. From a practical utility point, a conventional API separator can handle such concentrations of oil present in the resulting oil laden water [30]. The regenerated column was then fed with the same oil-in-water emulsion. Fig. 4 shows the plot of the ratio of effluent to influent oil concentration vs. bed volume. Thomas model equations and parameters k_T and q_o are shown in Table 2. As in the

first cycle, the nonlinear regression analysis provided higher correlation coefficient ($r > 0.9$) for all the three oils. The value of q_o obtained was 2.5, 0.03, and 0.5 mg/g for SMO, CO, and Bright-Edge 80, respectively. However, it may be noted that the correlation coefficient was much lower than that obtained for the first cycle. Under the effluent pH and other similar operation conditions, q_o value in the second cycle should not generally exceed the one in the first cycle [31]. It is possible that DI water used for desorption may not have regenerated all of the adsorbed oil from the bed completely resulting in a decreased number of adsorption sites available for the next adsorption cycle. Therefore, the regenerated biomass may have had a lower adsorption capacity compared to virgin biomass beads. This might be the case in this study; however, further investigation is necessary. Nevertheless, it could be seen that the regenerated beads still had the capability to adsorb oil.

4. Conclusions

Five kinetic models were used to predict the breakthrough curves and to determine the characteristic parameters of the column useful for process design. Most models were found suitable for describing the whole or a definite part of the dynamic behavior of the column. The Wolborska model described the initial part of the breakthrough curve. The Belter model reasonably predicted the experimental data. The breakthrough curves were not described well by the modified Chu model equations. The simulation of the whole breakthrough curve was better reflected by the Thomas, Yan, and Yoon Nelson models.

Acknowledgement

The authors would like to thank the Natural Sciences and Engineering Research Council of Canada for financial support for the study through a grant to the second author.

References

[1] E. Lobos-Moysa, M. Bodzak, Application of hybrid biological techniques to the treatment of municipal wastewater containing oils and fats, Desalin. Water Treat. 46 (2012) 32–37.
[2] A. Ummadisingu, S. Gupta, Characteristics and kinetics study of chitosan from seafood industry waste for oil spill cleanup, Desalin. Water Treat. 44 (2012) 44–51.
[3] A.L. Ahmad, S. Sumathi, B.H. Hameed, Adsorption of residue oil from palm oil mill effluent using powder and flake chitosan: Equilibrium and kinetic studies, Water Res. 39 (2005) 2483–2494.
[4] B. Volesky, Biosorption of Heavy Metals, CRC Press, Boca Raton, FL, 1993.
[5] A. Srinivasan, T. Viraraghavan, Biological processes for removal of oil from wastewater: A review, Fresenius Environ. Bull. 16(12a) (2007) 1532–1543.
[6] A. Srinivasan, T. Viraraghavan, Oil removal from water using biomaterials, Bioresour. Technol. 101(17) (2010) 6594–6600.
[7] A. Kapoor, T. Viraraghavan, Removal of heavy metals from aqueous solutions using immobilized fungal biomass in continuous mode, Water Res. 32(6) (1998) 1968–1977.
[8] G. Yan, T. Viraraghavan, Effect of pretreatment on the bioadsorption of heavy metals on *Mucor rouxii*, Water SA 26(1) (2000) 119–124.
[9] M. Tsezos, Engineering aspects of metal binding by biomass, In: H.L. Ehrlich, C.L. Brierley (Eds.), Microbial Mineral Recovery, McGraw-Hill, New York, NY, 1990 pp. 325–340.
[10] A. Srinivasan, T. Viraraghavan, K.T.W. Ng, Coalescence/filtration of an oil-in water emulsion in an immobilized *Mucor rouxii* biomass bed, Sep. Sci. Technol. 47 (2012) 2241–2249.
[11] N. Biswas, Electrochemical Treatment of Oil Emulsions, MASc Thesis. Department of Civil Engineering, University of Ottawa, Ottawa, Canada, 1973.
[12] A. Srinivasan, T. Viraraghavan, Removal of oil by walnut shell media, Bioresour. Technol. 99 (2008) 8217–8220.
[13] S. Bartnicki-Garcia, W.Y. Nickerson, Isolation, composition and structure of cell walls of filamentous and yeast-like forms of *Mucor rouxii*, Biochim. Biophys. Acta 58 (1962) 102–119.
[14] R.A.A. Muzzarelli, P. Illari, R. Tarsi, B. Dubini, W. Xia, Chitosan from *Absidia coerulea*, Carbohydr. Polym. 25 (1994) 45–50.
[15] K. Chu, Improved fixed bed models for metal biosorption, Chem. Eng. J. 97 (2004) 233–239.
[16] F. Pagnanelli, Equilibrium, kinetic and dynamic modeling of biosorption processes, In: P. Kotrba, M. Mackova, T. Macek (Eds.), Microbial Biosorption of Metals, Springer, Heidelberg, 2011, pp. 59–120.
[17] D.O. Cooney, Adsorption Design for Wastewater Treatment, CRC Press, Boca Raton, Fl, 1999.
[18] T. Viraraghavan, G.N. Mathavan, Peat filtration for oil removal, Proceedings of the 1989 Specialty Conference, Environmental Engineering Division, ASCE, Ausin, TX, July 10–12 (1989) 635–642.
[19] H. Moazed, T. Viraraghavan, Organo-clay anthracite filtration for oil removal, J. Can. Pet. Technol. 49(9) (2001) 37–42.
[20] D. Mysore, T. Viraraghavan, Y-C. Jin, Vermiculite filtration for removal of oil from water, Pract. Periodical Hazard. Toxic Radioact. Waste Manage. 10(3) (2006) 156–161.
[21] Statistica, Statistica for Windows, Release 5.1, Statsoft Inc., Tulsa, OK, 1997.
[22] H.C. Thomas, Chromatography: A problem in kinetics, Ann. N.Y. Acad. Sci. 49 (1948) 161–182.
[23] T.M. Reynolds, P.A. Richards, Unit Operations and Processes in Environmental Engineering, PWS, Boston, MA, 1996.
[24] G. Yan, T. Viraraghavan, M. Chen, A new model for heavy metal removal in a biosorption column, Adsorpt. Sci. Technol. 19(1) (2001) 25–43.
[25] P.A. Belter, E.L. Cussler, W.-S. Hu, Bioseparations: Downstream Processing for Biotechnology, Wiley, New York, NY, 1998.
[26] Y.H. Yoon, J.H. Nelson, Application of gas adsorption kinetics. I. A theoretical model for respirator cartridge service time, Am. Ind. Hyg. Assoc. J. 45 (1984) 509–516.
[27] A. Wolborska, Adsorption on activated carbon of *p*-nitrophenol from aqueous solution, Water Res. 23 (1989) 85–91.
[28] P. Lodeiro, R. Herrero, M.E. Sastre de Vicente, The use of protonated *Sargassum muticum* as biosorbent for cadmium removal in a fixed-bed column, J. Hazard. Mat. B137 (2006) 244–253.
[29] G. Bohart, E.N. Adams, Some aspects of the behavior of charcoal with respect to chlorine, J. Am. Chem. Soc. 42 (1920) 523–544.
[30] J.A. Aruldoss, T. Viraraghavan, Toxicity testing of refinery wastewater using Microtox, Bull. Environ. Contam. Toxicol. 60 (1998) 456–463.
[31] G. Yan, T. Viraraghavan, Heavy metal removal in a biosorption column by immobilized *M. rouxii* biomass, Bioresour. Technol. 78 (2001) 243–249.